Therapeutic and Diagnostic Algorithm for Patients with Obstructive Jaundice Based on the Estimation of the Optical Characteristics of the Liver and Bile

Elena V. Potapova[1*], Ksenia Y. Kandurova[1], Vadim N. Prizemin[1], Dmitry S. Sumin[2], and Andrian V. Mamoshin[1,2]

[1] Research and Development Center of Biomedical Photonics, 95 Komsomolskaya str., Orel State University, Orel 302026, Russian Federation

[2] Orel Regional Clinical Hospital, 10 Pobedy Blvd., Orel 302028, Russian Federation

*e-mail: potapova_ev_ogu@mail.ru

Abstract. Timely detection and prognosis of liver failure play an important role in improving treatment outcomes for patients with biliary obstruction. The study describes the use of optical biopsy methods to determine the functional state of the liver in patients with obstructive jaundice syndrome during and after antegrade biliary decompression. Fluorescence spectroscopy method allowed us to detect the patients suffering from severe liver failure during biliary drainage with high sensitivity, specificity, and accuracy (0.88, 0.98, and 0.96) to provide emergency treatment by extracorporeal detoxification methods. Raman spectroscopy method was proposed to be used to obtain additional diagnostic information on the recovery of excretory function of the liver to determine the possibility of transition to the next stage of treatment of the underlying disease. The scheme of treatment and diagnostic algorithm is proposed, which shows the position of optical diagnostic methods in the standard treatment protocol of patients with obstructive jaundice of different etiology. © 2024 Journal of Biomedical Photonics & Engineering.

Keywords: liver; obstructive jaundice; liver failure; decompression of bile ducts; optical biopsy; fluorescence spectroscopy; Raman spectroscopy; bile.

Paper #9149 received 8 Aug 2024; revised manuscript received 18 Sep 2024; accepted for publication 19 Sep 2024; published online 14 Oct 2024. doi: 10.18287/JBPE24.10.040304.

1 Introduction

Diagnosis and treatment of hepatopancreaticoduodenal diseases complicated by biliary obstruction remain an urgent problem in medicine. The number of patients with obstructive jaundice (OJ) of various etiologies is increasing every year, mainly due to changes in lifestyle and diet. OJ is a syndrome that develops as a result of impaired bile outflow through the intrahepatic and extrahepatic biliary ducts to the duodenum [1]. Biliary obstruction can be caused by cholelithiasis, inflammatory processes, benign and malignant diseases of hepatopancreaticoduodenal organs. One of the key factors worsening the prognosis of patients with OJ syndrome is the development of liver disorders based on hepatocyte dysfunction. Disruption of bile flow leads to accumulation of bile acids, bilirubin, and other metabolites in the liver and systemic circulation, resulting in the development of liver failure (LF) [2–4]. Increasing hyperbilirubinemia and functional LF cause pathological disorders in the whole organism, including vital organs and systems such as brain, kidneys, intestines, immune system, and others.

Surgical treatment in the presence of hyperbilirubinemia increases the risk of intra- and postoperative complications, so the treatment of patients with OJ syndrome is usually performed in two stages within the concept of preoperative biliary drainage [5]. In this approach, cholestasis is treated with minimally invasive procedures, followed by radical surgery after bilirubinemia resolves [6]. The placement of external, external-internal, or internal drainage systems is aimed at

early decompression of bile ducts, adequate, predictable, manageable and effective temporary or permanent biliary outflow and is the main way of temporary or definitive treatment of OJ, interruption of LF progression and prevention of complications development [7, 8]. However, LF may progress despite the drainage of the bile ducts in some clinical situations [9]. This is due to the fact that some patients have quite severe LF, and decompression procedures not only do not contribute to a rapid recovery, but actually aggravate the situation and require the use of extracorporeal hemocorrection methods or, in particularly severe cases, immediate intensive therapy for progressive LF. Thus, the success of treatment in patients with OJ syndrome depends significantly on the functional state of the liver [10, 11]. Clinical picture, common laboratory, and instrumental parameters of liver dysfunction developed due to OJ do not always correspond to the degree of liver damage, which requires further search for criteria to assess the severity of the condition of such patients [12].

As mentioned above, the development of biliary hypertension is one of the causes of impaired blood supply to the liver, resulting in damage to the membranes of hepatocytes and cholangiocytes. Accumulation of bilirubin and bile acids leads to inhibition of oxidative phosphorylation and antioxidant defenses of the liver, decrease of bioenergetic processes in mitochondria of hepatocytes [13]. As a result, significant impairment of oxygen utilization by cells is observed, which leads to pronounced tissue hypoxia of the liver. The degree and speed of pathological changes in liver tissue depend on the rate of increase in biliary hypertension, microcirculatory disturbance, tissue hypoxia, presence of inflammation in ducts and duration of disease [14]. It is also known that the composition of bile is closely related to the clinical severity, progression and prognosis of liver diseases, and its components can be reliable diagnostic and prognostic markers of the functional state of the organ [15–18].

Optical methods are characterized by high sensitivity to metabolic and biochemical changes in biological tissues and fluids [19–21]. One of the optical biopsy techniques widely used to monitor cellular and tissue metabolism in the liver parenchyma is fluorescence spectroscopy (FS) [22–26]. In previous work, we have shown that the use of deconvolution analysis of FS spectra allows us to identify the contribution of fluorophores reflecting changes in the liver of OJ patients [27]. Such fluorophores include NAD(P)H, flavins, bilirubin, vitamin A, protoporphyrins, and lipofuscin. Raman spectroscopy (RS) is widely used for highly sensitive physicochemical analysis of biological fluids [28]. Previously, we have shown that the determination of bilirubin concentration in bile obtained through the drainage catheter by RS allowed us to predict the recovery of excretory function of the liver and the dynamics of recovery of OJ patients after antegrade decompression of biliary tracts [29].

The aim of this work was to retrospectively study patients with OJ syndrome, different degrees of LF, and different dynamics of the postoperative period after antegrade biliary decompression, including the assessment of the functional state of the liver parenchyma by FS and bile composition by RS, as well as to develop a therapeutic and diagnostic algorithm including optical diagnostic methods in the standard protocol of treatment of OJ patients.

2 Materials and Methods

2.1 Object of Study

The study included 40 patients (66 ± 13 years) with OJ syndrome of different etiology (malignant tumors of the hepatopancreaticoduodenal area – 30 patients, gallstone disease – 8 patients, pancreatic head cyst with compression of the common bile duct – 2 patients). All patients underwent external percutaneous transhepatic cholangiostomy. According to clinical and laboratory parameters (results of blood biochemical analysis – the level of bilirubin fractions, alkaline phosphatase (ALP), alanine transaminase (ALT), aspartate transaminase (AST), creatinine, urea and total protein) before biliary decompression and the results of dynamic follow-up after the procedure, the patients were retrospectively divided into groups with positive (n=33) and negative (n=7) dynamics of the course of the postoperative period. In addition, it was possible to obtain bile samples from the common bile duct of 3 other patients after surgery for cholelithiasis. These patients did not have OJ syndrome and had a drainage catheter placed, so they could be considered as a control group without violations of the functional state of the liver. All studies were conducted in accordance with the Declaration of Helsinki of 1964 and its subsequent amendments and were approved by the local bioethics committee of Orel State University (Protocol № 28 dated 31.05.2023). All volunteers gave their informed consent for the study.

Fluorescence spectra were recorded at 1 or 2 points in the liver parenchyma near the bile ducts after creating primary access to the biliary tree under ultrasound and X-ray control. The total amount of measured spectra used for further analysis included 40 measurements for the positive dynamics group and 8 measurements for the negative dynamics group. Bile sampling for the study of optical properties by RS was performed during antegrade decompression of the biliary system by puncture needle and then every 3 days through the cholangiostomy drainage catheter. Reference samples for the control group were obtained through the drainage catheter 5 days after surgery.

2.2 Experimental Setup

Fluorescence spectra were recorded using the FS channel of a specially designed optical biopsy device [27]. Autofluorescence was excited at wavelengths of 365 nm and 450 nm. Fluorescence spectra were recorded using a CCD spectrometer in the 350−1000 nm range after attenuation of backscattered radiation from the sources. The optical radiation was transmitted through a small

diameter 1 mm fiber optic probe. The exposure time for measuring a spectrum was 1.5 s. For each patient, 5 fluorescence spectra were recorded at each wavelength at 1−2 study points and then averaged for further processing.

The study of the spectral characteristics of bile by RS was performed using the setup described in Ref. [29]. The volume of sample placed in the measurement cuvette was 5 ml. For each sample, 3 Raman spectra were recorded and averaged. In order to obtain Raman spectra of bile with a high signal-to-noise ratio, an exposure time of 90 s was chosen based on preliminary experiments. To reduce the contribution of fluorescence intensity to the total signal and to avoid photobleaching of the sample, the power of the 785 nm laser source was set to 16.5 mW.

2.3 Processing of Experimental Data

The processing of the signals recorded by FS in the liver parenchyma was performed in several steps. The averaged fluorescence spectra were smoothed with the Savitzky-Golay filter to remove noise but not to affect the shape of the spectra. The smoothed spectra were normalized from 0 to 100. The next step involved a non-linear deconvolution procedure based on the Levenberg-Marquardt algorithm to calculate combinations of Gaussian curves reflecting the contribution of each fluorophore to the total signal obtained from the liver tissue.

The fluorescence spectra were characterized by Gaussian curves related to the fluorescence of the following substances (Fig. 1(a, c)): collagen and elastin (curve 1), NAD(P)H (2) - reduced forms of nicotinamideneadenine dinucleotide (NADN) and nicotinamideneadenine dinucleotide phosphate (NADPH), free fatty acids (3), vitamin A (4), bilirubin (5, 7), flavins (6), lipofuscin (8), and porphyrins (9, 10). The number of curves, their central wavelengths and full width at half maximum values were initially selected from literature data on fluorophores of liver parenchyma [27] and then adjusted empirically to provide the best possible fit to the measured spectra. Parameters analyzed included peak heights and proportions of areas under Gaussian curves in the total area of the fluorescence spectra.

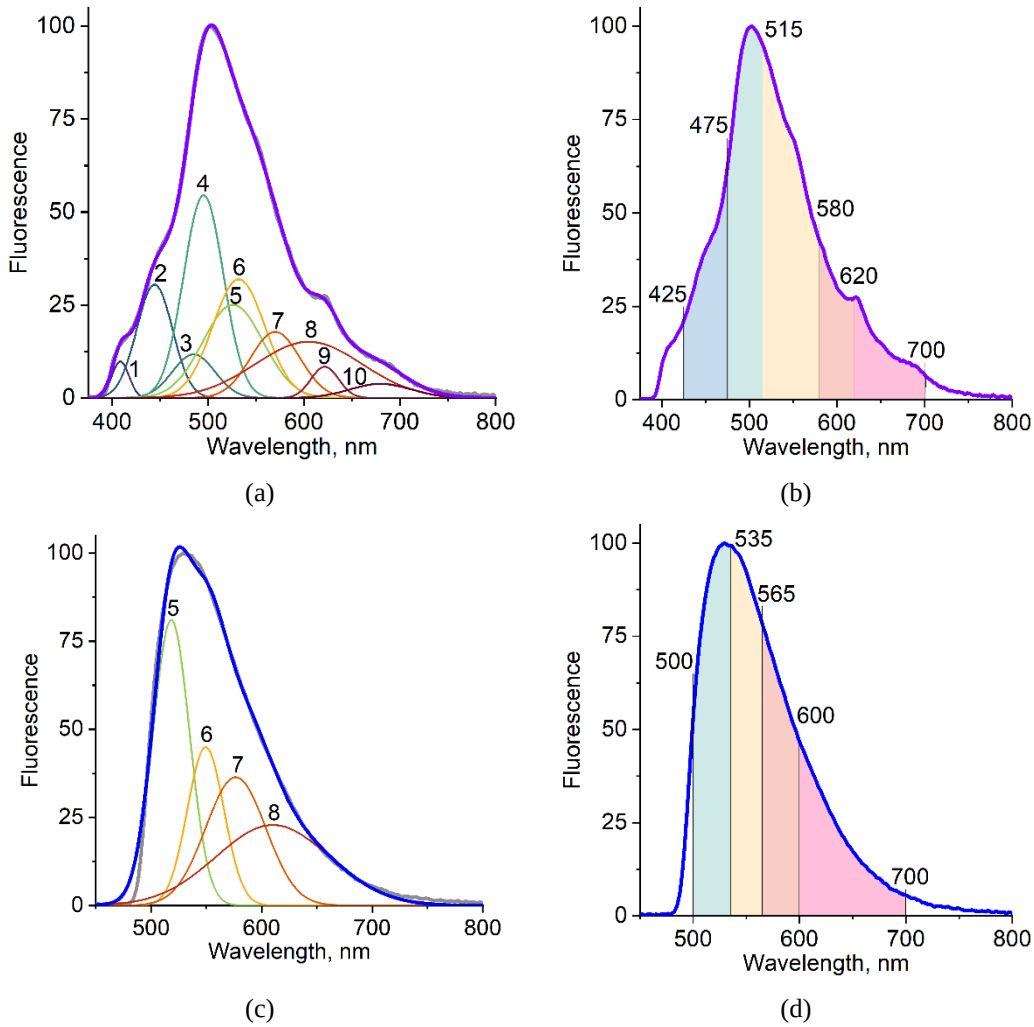

Fig. 1 Fluorescence spectra parameters calculated for analyzing: (a) fluorophores curves for 365 nm excitation wavelength, (b) fluorophores curves for 450 nm excitation wavelength, (c) bands for calculating areas under 365 nm spectrum, (d) bands for calculating areas under 450 nm spectrum.

In addition, the areas under the spectral curves in different spectral bands were calculated to take into account the simultaneous contribution of fluorophores with overlapping fluorescence spectra (Fig. 1(b, d)), as well as the areas of the spectra before and after the average wavelength of maximum fluorescence intensity (425−515 and 515−700 nm for the 365 nm excitation channel; 500−535 and 535−700 nm for the 450 nm excitation channel). Statistical significance of differences between groups was tested using the non-parametric Mann-Whitney *U* test due to limited sample size and lack of confirmed normal distribution of results in all compared samples.

The identified differences were used to select combinations of parameters promising for further development of a classifier to assess the functional state of the liver and identify severe LF in OJ patients. A linear discriminant analysis (LDA) approach was used to build a classification model and identify the features that best separate patients with OJ syndrome according to the expected positive or negative dynamics of the postoperative period after minimally invasive biliary drainage.

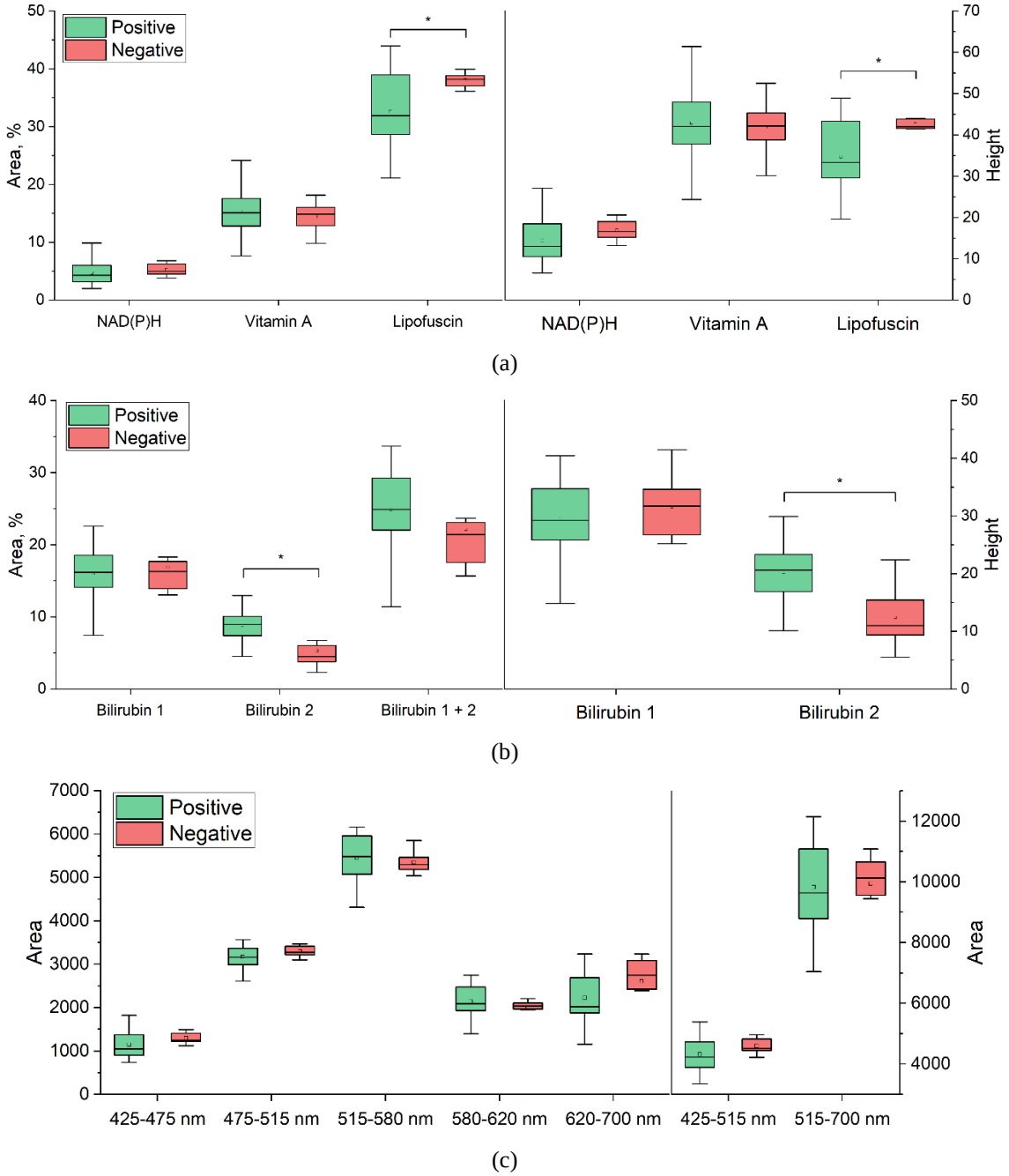

Fig. 2 Comparison of the parameters obtained by FS at 365 nm excitation: (a, b) percentage of the area under the Gaussian curves and their peaks heights for major liver tissue fluorophores, (c) areas under the spectra curve in different wavelength ranges. Statistically significant differences for *p < 0.05.

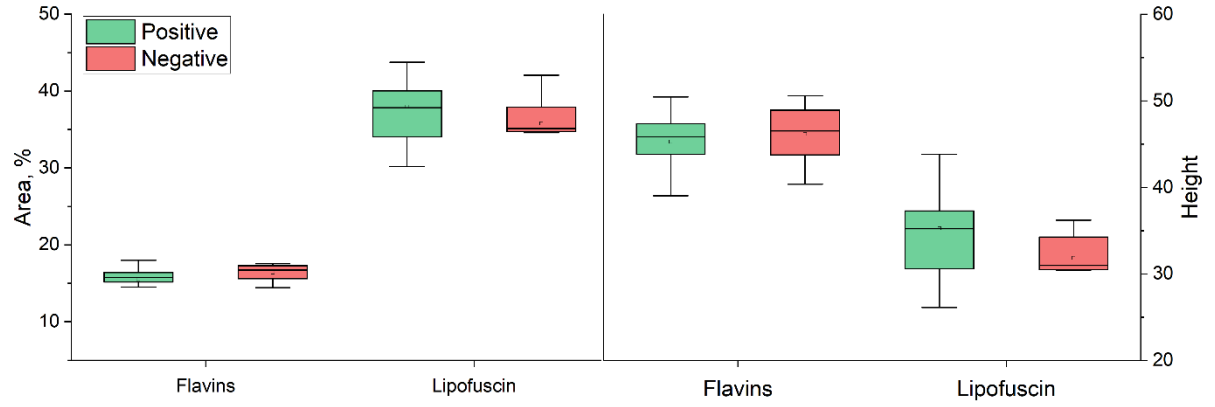

(a)

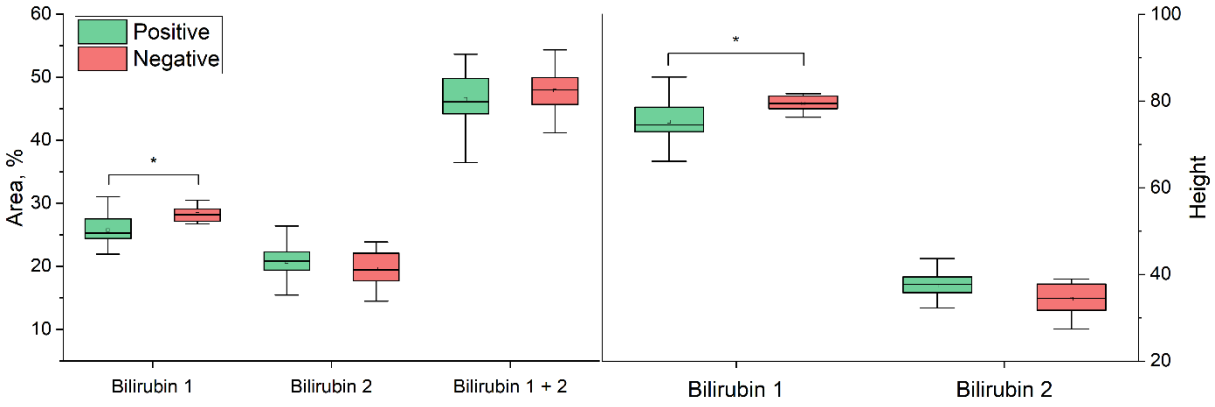

(b)

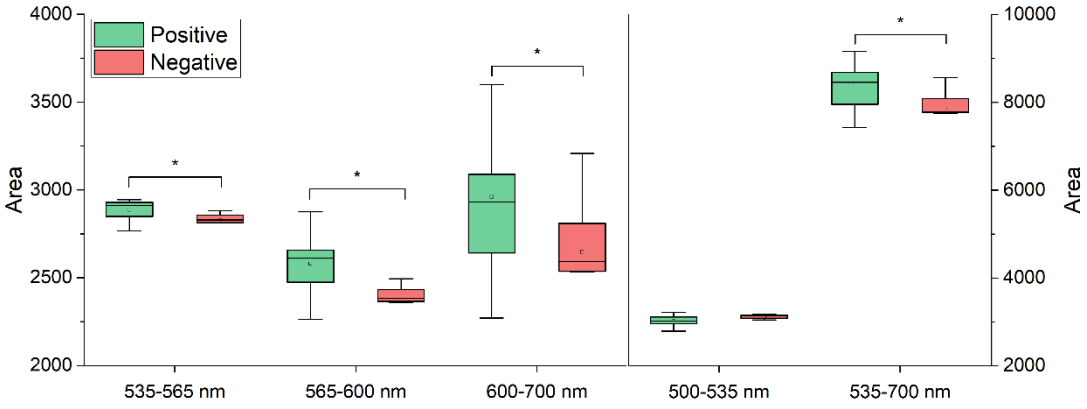

(c)

Fig. 3 Comparison of the parameters obtained by FS at 450 nm excitation: (a, b) percentage of the area under the Gaussian curves and their peaks heights for major liver tissue fluorophores, (c) areas under the spectra curve in different wavelength ranges. Statistically significant differences for *p < 0.05.

The result of LDA is the discriminant function, which should provide high sensitivity and specificity and an acceptable level of type 1 error (probability of a false negative result). The discriminant function is described by the following Eq.:

$$f(x) = \sum_1^n a_i x_i + c,$$

where $X = (x_1,\ldots,x_n)$ – vector of discriminant variables; $a = (a_1,\ldots,a_n)$ – vector of discriminant function coefficients; n – number of variables; c – a constant term.

The diagnostic criterion is a classification model as a discriminant function that allows us to classify the presence or absence of negative dynamics of the patient's condition after biliary decompression. To develop the diagnostic criterion, we calculated the vector of discriminant function coefficients and its constant term for each combination of discriminant variables. To select the most appropriate criterion for this diagnostic task, the sensitivity (proportion of true positive cases of negative dynamics), specificity (proportion of true negative cases), and accuracy (proportion of correctly predicted

cases) were evaluated, as well as the area under the error curve (AUC).

During RS spectra processing, the fluorescence background was removed by fitting the fluorescence spectrum using a polynomial approximation of the obtained data. The polynomial degree was set to 10 to provide the best possible fit according to the literature and empirical adjustments [30, 31]. The spectra were smoothed by the Savitsky-Golay filter with the following filter parameters: 15 number of sliding window points, 3 polynomial degree. The part of the spectrum in the 1000−1800 cm^{-1} range was analyzed. Detection of bilirubin was carried out in the following spectral bands: 1258−1264 cm^{-1} and 1615−1620 cm^{-1} [32].

All data processing was performed using OriginPro 2021 software.

3 Results

Fig. 2 shows the results of the comparison of the calculated fluorescence parameters under excitation at 365 nm for the two groups of patients analyzed. Despite the small number of patients who remained in the most severe condition after biliary decompression, changes in the curves and spectral areas reflecting the content of certain fluorophores were observed mainly in relation to bilirubin and lipofuscin.

The data obtained at 450 nm (Fig. 3) were characterized by statistically significant differences in the areas of the spectrum for almost all bands, which may be due in part to the optical properties of bilirubin, which has a higher absorption at 450 nm.

Table 1 shows the results of LDA for dividing the data into two groups (patients with positive and negative state dynamics after biliary decompression) for the pairs of discriminant variables with the highest sensitivity, specificity, and accuracy scores.

In order to achieve the highest sensitivity, specificity, and accuracy for all the methods used, the discriminant function based on the values of the height of the Gaussian curve of lipofuscin in the 365 nm spectrum $H_{lipofuscin}^{365\,nm}$ and the area of the 450 nm spectrum in the range of 565−600 nm $A_{565-600\,nm}^{450\,nm}$ was chosen as the most acceptable. As a result, the discriminant function of the classification model based on the combinations of parameters obtained by the FS method at 365 nm and 450 nm wavelengths is as follows:

$$f(x) = 0.28 \cdot H_{lipofuscin}^{365\,nm} - 0.02 \cdot A_{565-600\,nm}^{450\,nm} + 48.33. \quad (2)$$

Table 1 Sensitivity and specificity values of the obtained discriminant functions.

Parameters	Variables				
	Area, $A_{bilirubin\,2}^{365\,nm}$	**Area,** $A_{bilirubin\,2}^{365\,nm}$	**Area,** $A_{bilirubin\,2}^{365\,nm}$	**Area,** $A_{lipofuscin}^{365\,nm}$	**Height,** $H_{lipofuscin}^{365\,nm}$
	Area, $A_{bilirubin\,1+\,bilirubin\,2}^{450\,nm}$	**Area,** $A_{565-600\,nm}^{450\,nm}$	**Area,** $A_{535-700\,nm}^{450\,nm}$	**Area,** $A_{565-600\,nm}^{450\,nm}$	**Area,** $A_{565-600\,nm}^{450\,nm}$
Sensitivity	0.88	0.88	0.88	0.88	0.88
Specificity	0.95	0.98	0.95	0.95	0.98
Accuracy	0.94	0.96	0.94	0.94	0.96
AUC	0.94	0.97	0.96	0.99	0.99

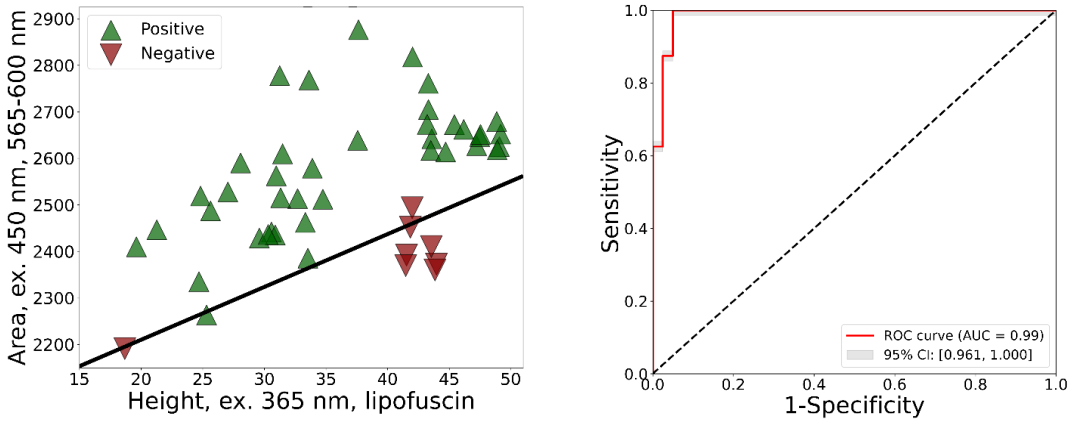

(a) (b)

Fig. 4 LDA results: (a) scatter plot of selected parameter values, (b) ROC curve with 95% confidence interval to evaluate the performance of the classification model.

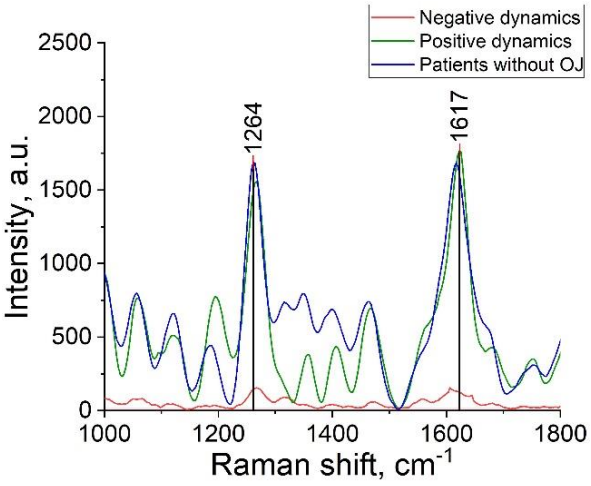

Fig. 5 Examples of Raman spectra of bile from patients without OJ syndrome, patients with negative and positive postoperative dynamics.

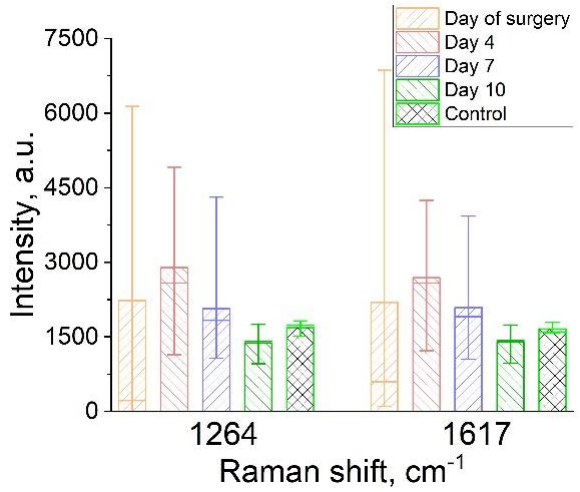

(a)

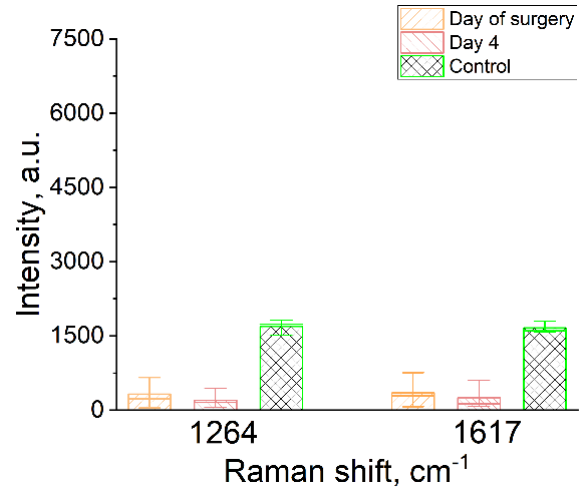

(b)

Fig. 6 Results of RS of patients in dynamics during the treatment: (a) patients with positive postoperative dynamics, (b) patients with negative postoperative dynamics.

Fig. 4 shows the LDA results as a scatter plot with a discriminant line dividing the experimental points into two groups. If the obtained experimental point lies above the discriminant line *f*, it is concluded that the patient will have positive dynamics of the state after biliary decompression, if the experimental point lies below the line *f* - that the patient will have negative dynamics in the postoperative period. Thus, we can conclude that the application of the FS method at 365 nm and 450 nm excitation wavelengths allows us to synthesize the decision rule for identifying patients with positive and negative dynamics of the state after biliary decompression with the probability of false negative results less than 0.2.

Fig. 5 shows typical Raman spectra of the bile samples from the control group as an example of normal bilirubin levels, as well as examples of Raman spectra of patients with suppressed (negative dynamics of the postoperative period) and restored excretory function of the liver (positive dynamics of the postoperative period) after antegrade decompression of biliary tracts. The Raman bands of bilirubin are clearly distinguishable in the spectra, which are caused by the bending and stretching of the C-H bond in the 1260 cm^{-1} wave shift region, and are associated with the bending of the C=H bond in the five-membered carbocycle in the 1615 cm^{-1} wave shift region [33]. Bilirubin peaks were analyzed in the spectral bands 1258−1264 cm^{-1} and 1615−1620 cm^{-1}. The maximum amplitude in the specified range was selected for each patient when processing the statistical data.

Fig. 6 shows Raman spectra of bile from OJ patients with different dynamics of the pathological process in the liver.

On the first day of the study, there was a great variation of data, which was associated with the different functional state of the liver of patients with OJ syndrome admitted to the hospital. Some patients had decreased secretory function due to biliary obstruction, while others had active production of bile in the lumen of biliary capillaries. There were also patients with initially normal excretory function of the liver, which correlated with their rather satisfactory condition according to blood biochemical analysis and general clinical evaluation of the patient's condition by a doctor [29].

Gradually, the patients of the first group showed normalization of Raman peaks in both studied bands (using the present configuration and operating modes of the diagnostic equipment) to the intensities of 1300−1600 a.u. (the level of bilirubin peaks in bile of conditionally healthy volunteers [29]), which correlated with clinical and laboratory data of recovery of liver function and general condition of patients).

The second group of patients showed signs of suppression of hepatic excretory function on the first day of the study. Three days later, it was found that the dynamics of changes in laboratory parameters in these patients indicated an unsatisfactory response of the liver parenchyma to antegrade biliary decompression, and it was necessary to add extracorporeal detoxification methods to the therapy. The patients were transferred to the intensive care unit.

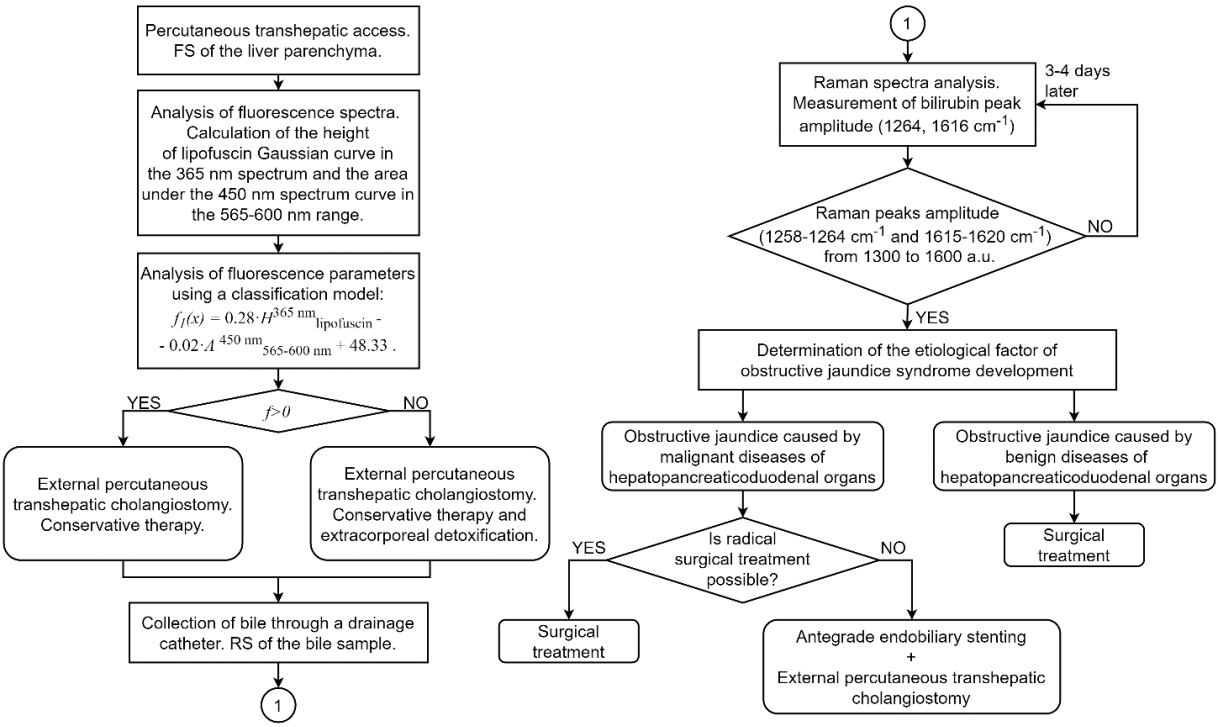

Fig. 7 The scheme of therapeutic and diagnostic algorithm including optical diagnostic methods in the standard treatment protocol for OJ patients.

Based on the retrospective study and established relationships between the course of postoperative period of OJ patients and optical characteristics of liver and bile, detected by optical diagnostic methods, a scheme of therapeutic and diagnostic algorithm was proposed, which shows the place of FS and RS in the standard treatment protocol for patients with OJ syndrome of various etiologies (Fig. 7).

Patients with OJ syndrome underwent standard treatment according to the recommended protocol upon admission to the hospital. During the creation of the primary antegrade transhepatic access, fluorescence spectra are recorded and subsequently processed to calculate diagnostic parameters included in the discriminant function. Based on data analysis, conclusions are drawn about the expected course of postoperative period of patients and the necessity of adding extracorporeal methods of hemocorrection to the therapy. Then, during the postoperative period, bile is collected through a drainage catheter and its optical properties are analyzed by RS method. If the amplitude of bilirubin peaks in spectral bands 1258−1264 cm^{-1} and 1615−1620 cm^{-1} is normalized to the values of 1300−1600 a. u., it is possible, if necessary, to perform additional diagnostic procedures to determine the etiological factor of the development of OJ syndrome and to proceed to the next stage of treatment of the main disease (oncology, gallstone disease, cysts, etc.).

4 Discussion

The retrospective study allowed to find out the relationship between the optical characteristics of the liver and bile with the course of the postoperative period after antegrade biliary decompression.

The assessment of the functional state of the liver using the FS method and the determination of the contributions of individual fluorophores demonstrate the possibility of obtaining new diagnostic information about changes in the structure and metabolic processes in the liver parenchyma. During the deconvolution analysis of the FS spectra, the highest values of fluorescence height were observed for the components characterizing fluorophores with emission spectra closest to the maximum of the whole spectrum, in particular vitamin A and bilirubin. A number of fluorophores, such as structural proteins and fatty acids, porphyrin derivatives (although increases were observed in some cases), made minor contributions to the spectra, but theirfluorescence could influence the area of individual segments that were also evaluated. Previous study has shown statistically significant changes in the fluorescence of NAD(P)H and flavins compared to results from patients without OJ, which is associated with significant impairment of hepatocyte function and development of hypoxia in OJ syndrome [27, 34]. The revealed changes did not show static significance among the groups of OJ patients, but there was a similar tendency of increase of their fluorescence contributions. It is known that with the increase of bilirubin content in liver tissues, oxidative phosphorylation and antioxidant defense disorders progress, and a decrease of bioenergetic processes in mitochondria of hepatocytes is observed, which is reflected in the obtained results [35].

The differences in the metabolic state are not as obvious as in the case of comparison with the patients without OJ, which suggests the search for potential diagnostic criteria among a larger number of fluorophores, which are noted to be used to assess changes in the progression of pathologies. Thus, when analyzing the areas of the fluorophore curves and the areas allocated under the curves of the initial spectrum in a certain range, a significant contribution of lipofuscin was noted, but without statistically significant differences. Lipofuscin, which contributes significantly to the fluorescence spectra, is considered to be a pigment that accumulates as a result of aging [36, 37], but some researchers consider it to be a marker of pathological processes in the liver, the accumulation of which depends on the degree of these processes [38, 39]. Accordingly, the level of this pigment can also be used to assess the metabolic state of cells, like other well-known biomarkers NAD(P)H and flavins [40]. Similarly, the results show an increase in the average contribution of lipofuscin fluorescence in the 365 nm fluorescence spectra for a group of patients with negative postoperative dynamics, which is associated with more severe hepatocyte damage and consequently with LF as a result of prolonged progression of OJ.

A decrease in the relative contribution of lipofuscin to the 450 nm fluorescence spectra may be due to an increase in the total contribution of bilirubin, despite a decrease in the contribution of the second peak of bilirubin fluorescence. Overall, the contribution of these fluorophores can be expected to cause statistically significant changes in the 450 nm fluorescence spectra and high accuracy rates when this parameter is used in various combinations of discriminant variables.

The developed algorithm based on the calculated parameters of FS (the height of the Gaussian curve of lipofuscin in the 365 nm spectrum and the area of the 450 nm spectrum in the range of 565−600 nm) showed high enough values of diagnostic effectiveness of the classifier: sensitivity 0.88, specificity 0.98, and accuracy 0.96 in identifying a group of patients requiring urgent intensive care.

The method of assessing the recovery of hepatic excretory function in patients with OJ syndrome by the intensity of Raman peaks of bilirubin is relatively simple and does not require any additional reagents. Based on the results obtained by RS, we can conclude that normalization of Raman peaks in both areas of the study (using the present configuration and operating modes of the diagnostic equipment) to intensities in the range of 1300−1600 a. u. correlates with clinical and laboratory data on recovery of liver function and general clinical condition of patients. This parameter can be taken into account when deciding on the next stage of OJ treatment.

The developed therapeutic and diagnostic algorithm considers the results of the application of two optical diagnostic methods and allows to develop individual treatment protocols for patients, taking into account the assessment of the functional state of the liver, determined by the optical characteristics of the liver parenchyma and bile. The developed approach may become the basis for improving the results of minimally invasive surgical procedures by identifying patients with severe LF and subjecting them to earlier intensive therapy, as well as by optimally determining the timing of transition to treatment of the patient's underlying disease, for example, lithoextraction in the case of cholelithiasis or tumor removal in the case of oncological etiology.

5 Conclusions

Most surgeons prefer a stepwise approach to surgical tactics in the treatment algorithm for patients with OJ syndrome. Despite numerous data confirming the efficacy of antegrade decompression procedures in resolving OJ syndrome, the question of widespread use of this type of minimally invasive drainage procedure remains controversial. This is due to the fact that in some patients with OJ syndrome with high and prolonged hyperbilirubinemia, removal of the biliary obstruction does not lead to an overall improvement of the condition and LF progression occurs.

The article proposes an approach for obtaining diagnostic information on the optical properties of the liver parenchyma and bile, which includes obtaining quantitative data on the contribution of fluorophores to the fluorescence spectra of liver tissues by decomposing the FS spectra using Gaussian curves and conducting studies on bile samples obtained during percutaneous transhepatic cholangiostomy and dynamically after biliary decompression in patients with OJ. The introduction of optical technologies into the standard algorithm for the treatment of patients with OJ syndrome of various etiologies will reduce the frequency of postoperative complications by identifying patients with severe LF, as well as predict the course of postoperative recovery of the functional state of the liver in order to plan the next stage of treatment.

We assume that this study will form the basis for the development of a point-of-care technology to assess the functional status of the liver and, in the future, lead to a correction of the recommendations for minimally invasive procedures in the biliary tract.

Acknowledgements

The research was supported by the Russian Science Foundation Grant No. 23-25-00487 (https://rscf.ru/en/project/23-25-00487/).

Disclosures

The authors declare that they have no conflict of interest.

References

1. J.-J. Liu, Y.-M. Sun, Y. Xu, H.-W. Mei, W. Guo, and Z.-L. Li, "Pathophysiological consequences and treatment strategy of obstructive jaundice," World Journal of Gastrointestinal Surgery 15(7), 1262–1276 (2023).
2. S.-Y. Cai, X. Ouyang, Y. Chen, C. J. Soroka, J. Wang, A. Mennone, Y. Wang, W. Z. Mehal, D. Jain, and J. L. Boyer, "Bile acids initiate cholestatic liver injury by triggering a hepatocyte-specific inflammatory response," JCI Insight 2(5), (2017).
3. A. Filipović, D. Mašulović, K. Gopčević, D. Galun, A. Igić, D. Bulatović, M. Zakošek, and T. Filipović, "Effect of Percutaneous Biliary Drainage on Enzyme Activity of Serum Matrix Metalloproteinase-9 in Patients with Malignant Hilar Obstructive Hyperbilirubinemia," Medicina 59(2), 336 (2023).
4. E. T. Pavlidis, T. E. Pavlidis, "Pathophysiological consequences of obstructive jaundice and perioperative management," Hepatobiliary & Pancreatic Diseases International 17(1), 17–21 (2018).
5. N. A. Van Der Gaag, J. J. Kloek, S. M. M. De Castro, O. R. C. Busch, T. M. Van Gulik, and D. J. Gouma, "Preoperative Biliary Drainage in Patients with Obstructive Jaundice: History and Current Status," Journal of Gastrointestinal Surgery 13(4), 814–820 (2009).
6. H. Moole, M. Bechtold, and S. R. Puli, "Efficacy of preoperative biliary drainage in malignant obstructive jaundice: a meta-analysis and systematic review," World Journal of Surgical Oncology 14(1), 182 (2016).
7. P. Watanapa, "Recovery patterns of liver function after complete and partial surgical biliary decompression," The American Journal of Surgery 171(2), 230–234 (1996).
8. O. M. Van Delden, J. S. Laméris, "Percutaneous drainage and stenting for palliation of malignant bile duct obstruction," European Radiology 18(3), 448–456 (2008).
9. C. Iacono, A. Ruzzenente, T. Campagnaro, L. Bortolasi, A. Valdegamberi, and A. Guglielmi, "Role of Preoperative Biliary Drainage in Jaundiced Patients Who Are Candidates for Pancreatoduodenectomy or Hepatic Resection: Highlights and Drawbacks," Annals of Surgery 257(2), 191–204 (2013).
10. S. Kumar, S. Masood, U. Srivastava, S. M. Madhavan, S. Chauhan, and A. Pandey, "Factors predicting recovery of liver function after percutaneous drainage in malignant biliary obstruction: the role of hospital-acquired biliary sepsis," Clinical and Experimental Hepatology 6(4), 295–303 (2020).
11. J. Sha, Y. Dong, and H. Niu, "A prospective study of risk factors for in-hospital mortality in patients with malignant obstructive jaundice undergoing percutaneous biliary drainage," Medicine 98(15), e15131 (2019).
12. F. Scheufele, L. Aichinger, C. Jäger, I. E. Demir, S. Schorn, E. Demir, M. Sargut, H. Friess, and G. O. Ceyhan, "INR and not bilirubin levels predict postoperative morbidity in patients with malignant obstructive jaundice," The American Journal of Surgery 222(5), 976–982 (2021).
13. C. Ercin, S. Bagci, Z. Yesilova, A. Aydin, A. Sayal, and G. Erdem, "Oxidative stress in extrahepatic cholestasis," The Anatolian Journal of Clinical Investigation 2(4), 150−154 (2008).
14. M. Tanaka, K. Tanaka, Y. Masaki, M. Miyazaki, M. Kato, K. Kotoh, M. Enjoji, M. Nakamuta, and R. Takayanagi, "Intrahepatic microcirculatory disorder, parenchymal hypoxia and NOX4 upregulation result in zonal differences in hepatocyte apoptosis following lipopolysaccharide- and D-galactosamine-induced acute liver failure in rats," International Journal of Molecular Medicine 33(2), 254–262 (2014).
15. A. Verma, V. Bhatnagar, S. Prakash, and A. Srivastava, "Analysis of bile in various hepatobiliary disease states: A pilot study," Journal of Indian Association of Pediatric Surgeons 19(3), 151−155 (2014).
16. M. L. Shiffman, H. J. Sugerman, J. M. Kellum, and E. W. Moore, "Changes in gallbladder bile composition following gallstone formation and weight reduction," Gastroenterology 103(1), 214–221 (1992).
17. A. P. M. Matton, Y. De Vries, L. C. Burlage, R. Van Rijn, M. Fujiyoshi, V. E. De Meijer, M. T. De Boer, R. H. J. De Kleine, H. J. Verkade, A. S. H. Gouw, T. Lisman, and R. J. Porte, "Biliary Bicarbonate, pH, and Glucose Are Suitable Biomarkers of Biliary Viability During Ex Situ Normothermic Machine Perfusion of Human Donor Livers," Transplantation 103(7), 1405–1413 (2019).
18. I. M. A. Brüggenwirth, R. J. Porte, and P. N. Martins, "Bile composition as a diagnostic and prognostic tool in liver transplantation," Liver Transplantation 26(9), 1177–1187 (2020).
19. S. Palmer, K. Litvinova, A. Dunaev, S. Fleming, D. McGloin, and G. Nabi, "Changes in autofluorescence based organoid model of muscle invasive urinary bladder cancer," Biomedical Optics Express 7(4), 1193−1200 (2016).
20. A. V. Dunaev, V. V. Dremin, E. A. Zherebtsov, I. E. Rafailov, K. S. Litvinova, S. G. Palmer, N. A. Stewart, S. G. Sokolovski, and E. U. Rafailov, "Individual variability analysis of fluorescence parameters measured in skin with different levels of nutritive blood flow," Medical Engineering & Physics 37(6), 574–583 (2015).
21. I. A. Bratchenko, D. N. Artemyev, O. O. Myakinin, Y. A. Khristoforova, A. A. Moryatov, S. V. Kozlov, and V. P. Zakharov, "Combined Raman and autofluorescence ex vivo diagnostics of skin cancer in near-infrared and visible regions," Journal of Biomedical Optics 22(2), 027005 (2017).
22. A. C. Croce, A. Ferrigno, G. Santin, V. M. Piccolini, G. Bottiroli, and M. Vairetti, "Autofluorescence of liver tissue and bile: Organ functionality monitoring during ischemia and reoxygenation," Lasers in Surgery and Medicine 46(5), 412–421 (2014).

23. A. C. Croce, A. Ferrigno, V. Bertone, V. M. Piccolini, C. Berardo, L. G. Di Pasqua, V. Rizzo, G. Bottiroli, and M. Vairetti, "Fatty liver oxidative events monitored by autofluorescence optical diagnosis: Comparison between subnormothermic machine perfusion and conventional cold storage preservation," Hepatology Research 47(7), 668–682 (2017).
24. V. Dremin, E. Potapova, E. Zherebtsov, K. Kandurova, V. Shupletsov, A. Alekseyev, A. Mamoshin, and A. Dunaev, "Optical percutaneous needle biopsy of the liver: a pilot animal and clinical study," Scientific Reports 10(1), 14200 (2020).
25. E. V. Potapova, E. A. Zherebtsov, V. V. Shupletsov, V. V. Dremin, K. Y. Kandurova, A. V. Mamoshin, A. Y. Abramov, and A. V. Dunaev, "Detection of NADH and NADPH levels in vivo identifies shift of glucose metabolism in cancer to energy production," The FEBS Journal 291(12), 2674–2682 (2024).
26. E. A. Zherebtsov, E. V. Potapova, A. V. Mamoshin, V. V. Shupletsov, K. Y. Kandurova, V. V. Dremin, A. Y. Abramov, and A. V. Dunaev, "Fluorescence lifetime needle optical biopsy discriminates hepatocellular carcinoma," Biomedical Optics Express 13(2), 633 (2022).
27. K. Y. Kandurova, D. S. Sumin, A. V. Mamoshin, and E. V. Potapova, "Deconvolution of the fluorescence spectra measured through a needle probe to assess the functional state of the liver," Lasers Surg Med 55(7), 690–701 (2023).
28. K. Kong, C. Kendall, N. Stone, and I. Notingher, "Raman spectroscopy for medical diagnostics — From in-vitro biofluid assays to in-vivo cancer detection," Advanced Drug Delivery Reviews 89, 121–134 (2015).
29. E. V. Potapova, V. N. Prizemin, D. S. Sumin, and A. V. Mamoshin, "Assessment of Bilirubin Concentrations in the Bile of Patients with Obstructive Jaundice by Raman Spectroscopy," Optics and Spectroscopy 132(2), 179–187 (2024).
30. J. Zhao, H. Lui, D. I. McLean, and H. Zeng, "Automated Autofluorescence Background Subtraction Algorithm for Biomedical Raman Spectroscopy," Applied Spectroscopy 61(11), 1225–1232 (2007).
31. L. A. Bratchenko, I. A. Bratchenko, D. N. Artemyev, A. A. Moryatov, J. V. Starikova, E. N. Tupikova, I. A. Platonov, S. V. Kozlov, and V. P. Zakharov, "Conventional Raman and surface-enhanced Raman spectroscopy of ascitic fluid," Journal of Physics: Conference Series 1368(2), 022032 (2019).
32. B. Yang, M. D. Morris, M. Xie, and D. A. Lightner, "Resonance Raman spectroscopy of bilirubins: band assignments and application to bilirubin/lipid complexation," Biochemistry 30(3), 688–694 (1991).
33. L. Ouyang, L. Yao, R. Tang, X. Yang, and L. Zhu, "Biomimetic point-of-care testing of trace free bilirubin in serum by using glucose selective capture and surface-enhanced Raman spectroscopy," Sensors and Actuators B: Chemical 340, 129941 (2021).
34. T. Okaya, K. Nakagawa, F. Kimura, H. Shimizu, H. Yoshidome, M. Ohtsuka, Y. Morita, and M. Miyazaki, "Obstructive jaundice impedes hepatic microcirculation in mice," Hepatogastroenterology 55(88), 2146–2150 (2008).
35. A. C. Croce, A. Ferrigno, C. Berardo, G. Bottiroli, M. Vairetti, and L. G. Di Pasqua, "Spectrofluorometric Analysis of Autofluorescing Components of Crude Serum from a Rat Liver Model of Ischemia and Reperfusion," Molecules 25(6), 1327 (2020).
36. U. T. Brunk, A. Terman, "Lipofuscin: mechanisms of age-related accumulation and influence on cell function," Free Radical Biology and Medicine 33(5), 611–619 (2002).
37. O.-D. Ilie, A. Ciobica, S. Riga, N. Dhunna, J. McKenna, I. Mavroudis, B. Doroftei, A.-M. Ciobanu, and D. Riga, "Mini-Review on Lipofuscin and Aging: Focusing on The Molecular Interface, The Biological Recycling Mechanism, Oxidative Stress, and The Gut-Brain Axis Functionality," Medicina 56(11), 626 (2020).
38. S. G. Hübscher, R. F. Harrison, "Portal lymphadenopathy associated with lipofuscin in chronic cholestatic liver disease," Journal of Clinical Pathology 42(11), 1160–1165 (1989).
39. M. Saif, W. J. Kwanten, J. A. Carr, I. X. Chen, J. M. Posada, A. Srivastava, J. Zhang, Y. Zheng, M. Pinter, S. Chatterjee, S. Softic, C. R. Kahn, K. Van Leyen, O. T. Bruns, R. K. Jain, and M. G. Bawendi, "Non-invasive monitoring of chronic liver disease via near-infrared and shortwave-infrared imaging of endogenous lipofuscin," Nature Biomedical Engineering 4(8), 801–813 (2020).
40. E. I. Lebedzeva, "Histological characteristics of lipofuscin in the liver of rats with experimental cirrhosis," Proceedings of the National Academy of Sciences of Belarus, Medical Series (2), 41–46 (2015). [in Russian]